Category UC-126

SAND88-1895
Unlimited Release
November 1988

MICROWAVE TRANSMISSION THROUGH STRATEGIC PETROLEUM RESERVE CRUDE OIL SAMPLES FROM BAYOU CHOCTAW CAVERNS

J. G. Castle
SPR Geotechnical Division
Sandia National Laboratories
Albuquerque, New Mexico 87185-5800

ABSTRACT

Transmission of microwave power at frequencies from 1 to 11 GHz has been observed through a short, slotted, coaxial line filled with crude oil from each of five wellhead samples collected at Bayou Choctaw (BC) and one sample from a West Hackberry cavern (WH105). An accurate model for the filled slotted line is used to derive the dielectric constant and loss tangent for each oil. The highest loss occurs in oil from BC19 whose loss tangent is 0.0103 at 1 GHz; the lowest, in WH105 whose loss tangent at 1 GHz is 0.0026. These data suggest favorable prospects for high-resolution radar mapping of SPR cavern walls. Sulphur compounds in the oil appear to be the major source of the microwave attenuation.

LIST OF FIGURES

A.2.1.2 Power Transmission, Air Filling..... A5
A.2.2.1 Reflections with Refined Oil LAX..... A7
A.2.2.2 Tranamiaaion with Refined oil LAX..... A8
A.2.3.1.1 Power Reflection with Oil Prom SPR Cavern BC15. A9
A.2.3.1.2 Power Reflection with Oil From SPR Cavern BC17. A9
A.2.3.1.3 Power Reflection with Oil *From* SPR Cavern BC18. A10
A.2.3.1.4 Power Reflection with Oil From SPR Cavern BC19. A10
A.2.3.1.5 Power Reflection with Oil *From* SPR Cavern BC20. All
A.2.3.1.6 Power Reflection with Oil From SPR Cavern WH105 All
A.2.3.2.1 Tranamisaion with Oil From SPR Cavern BC15..... Al2
A.2.3.2.2 Tranamiaaion with Oil From SPR Cavern BC17..... Al3
A.2.3.2.3 Tranamiaaion with Oil From SPR Cavern BC18..... Al3
A.2.3.2.4 Tranamiaaion with Oil From SPR Cavern BC19..... Al4
A.2.3.2.5 Transmission *with* Oil *From* SPR Cavern BC20..... A14
A.2.3.2.6 *Transmission* with Oil From SPR Cavern WH105.... A15
B.2 Test Of *Fit* Of Calculated $|S_{21}|^2$ for Air..... B5
B.3.1 Calculated $|S_{21}|^2$ for LOW-LOSS Refined Oil..... B6
B.3.2 Test of Fit of Calculated $|S_{21}|^2$ for LAX Oil.... B7
B.4.1.1 Test of Fit in SPR Crude Oil from BC15..... B7
B.4.1.2 Test of Fit in *SPR* Crud8 Oil from BC17..... B8
B.4.1.3 Test of Fit in SPR Crud8 Oil from BC18..... B8
B.4.1.4 Teat of Fit in SPR Crud8 Oil from BC19..... B9
B.4.1.5 *Test* of Fit in SPR Crud8 Oil from BC20..... B9
B.4.1.6 Test of Fit in SPR Crude Oil from WH105..... B10

1. INTRODUCTION

1.1 Monitoring SPR Caverns Dimensions

Adequate monitoring of the oil storage caverns within the U.S. Strategic Petroleum Reserve (SPR) involves making the measurements necessary to evaluate cavern stability and, if possible, to inventory the oil contained on an appropriate schedule.[1-5] Daily readings of wellhead pressures are being used to monitor the normal volume decrease in all SPR caverns. Monitoring of SPR cavern dimensions over the long-term will require mapping of wall conditions in SPR caverns and will confirm the crude oil inventory at SPR.

A typical SPR cavern is a large carrot-shaped oil-filled chamber, roughly 200 feet in diameter and 2000 feet tall.1 At the start of this test, it appeared that there might be two technologies - radar and sonar - capable of mapping irregularities in the cavern oil-salt interface (wall) with enough resolution at a SPR cavern wall to measure wall contour and dimensions.[5-8] However, both radar and sonar signals are significantly attenuated by the crude oil, making the demonstration of mapping feasibility a significant challenge.

To be useful, a map of a SPR cavern wall will need to resolve an area of the cavern wall which is only a few feet across. To do this, sonar with a single transducer will need to be parametric, i.e., to produce a low-frequency sonar carrier by nonlinear generation from two high-power, high-frequency primary waves. For useful wall resolution by radar, the radar antenna will need to be a broadside array of coherent horns spanning both horizontally and vertically some twenty wavelengths. To get sufficiently strong radar echos, the attenuation in the oil must be low. The results of the present study indicate that mapping of most SPR cavern walls with useful resolution is feasible by radar at one GHz; numerical estimates of expected signal-to-noise will be presented in a separate report under preparation.7

No information is available in the public literature on microwave losses in crude oils.9 Therefore, the laboratory measurements were undertaken as the initial step toward understanding the extent to which crude oils absorb microwave energy.

1.2 Scope of This Test Report

The purpose of this report is to summarize the results observed for microwave transmission through a coaxial sample holder for six oil samples from SPR caverns. The oil samples were obtained at the wellhead of each of five caverns at Bayou Choctaw (BC) and *one* West Hackberry (WH) cavern.

The observed transmission data are interpreted in terms of the two parts of the dielectric permittivity of the oil sample: the dielectric constant ε_r', and the loss tangent $\tan\delta$. The latter is defined as the ratio of the imaginary part to the real part of the dielectric permittivity.[10] $\tan\delta$ values obtained in this study are listed from 1 to 10 GHz. Since the power lost in travelling one wavelength equals 27 dB times the value of tan6 at the wave frequency, oil with lower values of tan6 supports better transmission..

Loss at microwave frequencies occurs primarily in the polar molecules in the crude oil. If water and alcohol are not dispersed in the oil, sulphur compounds in the oil are the source of most of the microwave loss.

1.2.1 Microwave S-Parameters of Holder Under Test

The transmission and reflection properties of any two-terminal linear network can be completely described by the four complex elements, called S-parameters, of the scattering matrix of the network at each frequency.10 The network we are concerned with in these measurements is the coaxial sample holder, whether it is empty *or* filled with an oil. The two S-parameters of interest in this study are: S_{21}, the transmitted voltage vector for unity-amplitude zero-phase input to Port 1, and S_{11}, the reflected

voltage vector for unity-amplitude zero-phase input to Port 1. The squares of these two S-parameters represent the power transmitted by and reflected from the sample holder, respectively.

Appendix A presents graphs of the measured values of $|S_{11}|^2$ and $|S_{21}|^2$ versus frequency. The dielectric constant ε_r' is obtained from the observed $|S_{11}|^2$ versus frequency for each oil. Then, the observed $|S_{21}|^2$ for the slotted holder filled with that oil is used to calculate the loss tangent at each frequency.

1.2.2 Accuracy of Loss Tangent Values

The manufacturer of the automatic network analyzer (ANA) used to observe S-parameters states the ANA accuracy conservatively and therefore disclaims any values of loss tangent as low as 0.1 as being inaccurate.10 Based on our measurements, we believe that the sensitivity and stability of the ANA used in the manner described in Appendix A permits reliable measurements of liquid loss tangents to much lower values.

Care was taken to confirm reproducibility to within 0.03 dB in transmission and to avoid any polar cleaning material. The uncertainty in the tan6 values calculated for these oils appears to be as low as $\pm$ 0.0002, as discussed in Appendices A and B.

2. OIL SAMPLES

Oil samples selected for this first test are five crudes from BC, and a very sweet crude sample from WH, probably from WH105. A refined laxative-grade mineral oil is used to validate the multiple-reflection model of the coaxial holder and to serve as a comparison reference in case other methods are to be used in measuring microwave losses in crude oils.

2.1 Crude Oils from Wellheads at Bayou Choctaw

A wellhead sample of -300 ml of crude was obtained in March 1988 from each of five caverns, namely, BC15, BC17, BC18, BC19,

and BC20. Viscosity of these samples ranged from nearly that of gasoline to that of corn syrup. Some of the pertinent chemical data from these caverns are given in Table 2.1, as a summary of the January 5, 1988, NIPER tests. NIPER stands for the National Institute for Petroleum Energy Research, the organization which currently analyzes the chemical makeup of oil samples taken from SPR caverns on a regular schedule.

Table 2.1 Contents *of* Crude Oil8 *Stored* in SPR Caverns

Values of concentration are the averages among several NIPER samples taken on 1/5/88 at different depths within each cavern. The numerical designations within the NIPER labels give the lower temperature limit of the range used for each API gravity cut used in the NIPER processing: RES = residual. No data were available for BC17.

NIPER Variable	Units	BC15	BC18	BC19	BC20
API		33.0	36.2	32.9	36.4
SPGR	g/cm3	0.860	0.847	0.861	0.843
CONCR		3.9	2.6	4.4	
NITR	Wt%	0.134	0.10	0.136	0.11
SULPHUR	Wt%	1.54	0.39	1.61	0.23
MERCAP	ppm	14 ± 6	7	39 ± 26	
Sulphur Concentrations within Distillate Fractions:					
SULWRES	Wt%	3.61	1.34	3.76	
SULW375	wt %	0.36	0.10	0.35	
SULW530	wt %		0.36	1.11	
SULW650	wt %	2.09	0.58	2.15	
Mercaptan Concentrations within Distillate Fractions:					
MERC5	ppm	19	5	33 ± 18	
MERC175	ppm	65	11	46 ± 21	
MERC250	ppm	129	33	113 ± 17	
MERC375	ppm	42	14	43 + 8	

2.2 The Sweetest Crud. Oil Sample

A sample from WH105 obtained several years ago was also used in this study. The latest revision of the SPR Configuration Chart shows WH105 oil having 0.2 wt % sulphur.

3. OBSERVATIONS

Transmission of low-level microwave power through a coaxial slotted line while it was filled by each oil was measured at frequencies from 1 GHz to 11 GHz in steps of 0.050 GHz. A calibrated automatic network analyzer was used to obtain values for each of the four S-parameters of the slotted line at each frequency. Details of the measurement process and the graphs recorded by the ANA are given in Appendix A.

3.1 Observations on Air-Filled Bolder

The air-filled holder was observed to have very low loss and weak reflections from 1 to 10 GHz. For example, $|S_{21}|^2$ equals -0.05 dB at 1 GHz, -0.11 dB at 3 GHz, and -0.26 dB at 10 GHz, as shown in Figure A2.1.

3.2 Observations on Low-Loss Refined Oil

Filling the holder with a liquid gives a strong reflection at each end of the liquid because of the abrupt change in impedance of the coaxial line. The principal dips in power transmission are due to destructive interference involving these two reflections.

When it was filled with clear laxative-grade mineral oil (LAX), the holder exhibited low loss with prominent dips in both transmission and reflection across the 1 to 11 GHz region. The period of 0.45 GHz in the dips is produced by the 23.4-cm length of oil having an $\varepsilon_r'_{LAX}$ of 2.1. Furthermore, the low loss is shown by the trace of the maxima in $|S_{21}|^2$ being -0.19 dB at 3 GHz

compared to -0.11 dB at 3 GHz with air. This gives a loss tangent equal to 0.0004 for LAX. The fitting process is discussed in Appendix B.

3.3 Observationa on Crude Oil Samples

The $|S_{11}|^2$ and $|S_{21}|^2$ were plotted by the ANA at each frequency step from 1 to 11 GHz for the holder filled with each of the crude oils from Bayou Choctaw and WH105. The ANA graphs presented in Appendix A were used to extract the values of transmission peaks (TP), which are listed in Table 3.3.

Table 3.3 EM Transmission Peaks Observed in SPR Crudes.

The transmission maxima are observed to have a constant period near 0.45 GHz for each oil. The value of the locus of the maxima in $|S_{21}|^2$ for each oil is listed at ten values of frequency for ease in comparison between oils.

f GHz	BC15B dB	BC17A dB	BC18D dB	BC19D dB	BC20B dB	WH105 dB
1	0.412	0.394	0.325	0.475	0.288	0.156
2	0.675	0.650	0.538	0.754	0.506	0.281
3	0.875	0.850	0.675	1.000	0.675	0.388
4	1.056	1.022	0.819	1.219	0.812	0.488
5	1.212	1.169	0.944	1.438	0.925	0.562
6	1.338	1.312	1.056	1.650	1.050	0.656
7	1.481	1.444	1.169	'1.862	1.156	0.738
8	1.600	1.575	1.278	2.075	1.256	0.825
9	1.712	1.688	1.394	2.288	1.350	0.909
10	1.850	1.800	1.500	2.506	1 . 450	0.994

4. ANALYSIS OF OBSERVATIONS

Calculated values are fitted to the observed values of $|S_{21}|^2$ and $|S_{11}|^2$ using the known properties of air and the coaxial holder and the unknown (adjustable) permittivity of the oil involved. The fitting process is presented in Appendix B.

compared to -0.11 dB at 3 GHz with air. This gives a loss tangent equal to 0.0004 for LAX. The fitting process is discussed in Appendix B.

3.3 Observationa on Crude Oil Samples

The $|S_{11}|^2$ and $|S_{21}|^2$ were plotted by the ANA at each frequency step from 1 to 11 GHz for the holder filled with each of the crude oils from Bayou Choctaw and WH105. The ANA graphs presented in Appendix A were used to extract the values of transmission peaks (TP), which are listed in Table 3.3.

Table 3.3 EM Transmission Peaks Observed in SPR Crudes.

The transmission maxima are observed to have a constant period near 0.45 GHz for each oil. The value of the locus of the maxima in $|S_{21}|^2$ for each oil is listed at ten values of frequency for ease in comparison between oils.

f GHz	BC15B dB	BC17A dB	BC18D dB	BC19D dB	BC20B dB	WH105 dB
1	0.412	0.394	0.325	0.475	0.288	0.156
2	0.675	0.650	0.538	0.754	0.506	0.281
3	0.875	0.850	0.675	1.000	0.675	0.388
4	1.056	1.022	0.819	1.219	0.812	0.488
5	1.212	1.169	0.944	1.438	0.925	0.562
6	1.338	1.312	1.056	1.650	1.050	0.656
7	1.481	1.444	1.169	'1.862	1.156	0.738
8	1.600	1.575	1.278	2.075	1.256	0.825
9	1.712	1.688	1.394	2.288	1.350	0.909
10	1.850	1.800	1.500	2.506	1 . 450	0.994

4. ANALYSIS OF OBSERVATIONS

Calculated values are fitted to the observed values of $|S_{21}|^2$ and $|S_{11}|^2$ using the known properties of air and the coaxial holder and the unknown (adjustable) permittivity of the oil involved. The fitting process is presented in Appendix B.

Properties of the holder are confirmed or determined by the observations with air filling. For example, most of the 0.11-dB loss at 3 GHz is due to the conduction currents within the metal walls of the 23.4-cm air chamber: the rest is from the two ferrite beads.

Assuming the presence of a pair of equal-sized air bubbles, one at each end of the thick laxative oil LAX, we were able to fit accurately all of the prominent features of both $|S_{11}|^2$ and $|S_{21}|^2$ by adjusting only the size of the bubbles (length and angle subtended) and the two quantities $\varepsilon_r'_{LAX}$ and $\tan\delta_{LAX}$. For example, the graph in Figure B3.1 displays the calculated $|S_{21}|^2$ which fits the observed $|S_{21}|^2$ in Figure A2.2.2 to within the thickness of the lines on the graphs.

Similarly, the only adjustable parameters in fitting the observations on each crude oil are:

$\varepsilon_r'_{oil}$,
the dimensions of any air bubble, and
$\tan\delta_{oil}$.

The thin oils trap no bubbles.

4.1 Dielectric Constant of Crude Oils

The dielectric constant for each crude oil is determined from the constant period of the dips observed in $|S_{11}|^2$ and $|S_{21}|^2$ as discussed in Appendix A2. The values found for $\varepsilon_r'_{oil}$ are listed in Table 4.1.

Table 4.1 **Microwave** Dielectric Constant of Crude oils

The real part of the relative **permittivity** was calculated from the regular period observed in the dips in $|S_{11}|^2$ from 1 to 10 GHz and then trimmed -1% in fitting to the dips observed in $|S_{21}|^2$. The ANA data are shown in Section A2.3 of Appendix A.

Cavern	$\varepsilon_r'_{oil}$	Uncertainty ±
BC15	2.22	**.01**
BC17	2.19	**.01**
BC18	2.17	**.01**
BC19	2.28	**.01**
BC20	2.180	**.005**
CRD1	2.335	ooq

4.2 Loss Tangents in Crude Oils

The loss tangent values used to calculate the $|S_{21}|^2$ that agree with the observed $|S_{21}|^2$ are listed in Table 4.2. The excellent quality of fit of the calculated $|S_{21}|^2$ to the observed values is shown graphically in Appendix B to be within ± 0.03 **dB.**

Table 4.2 **Microwave** Loss **Tangent** for Crude oils

The loss tangent is calculated at each frequency by Equation (4.3) using the model parameters listed at the bottom of the column for each oil. Substitution of each value of loss tangent produces a calculated $|S_{21}|^2$ which agrees with the observed one within 0.03 **dB.**

f **GHz**	Cavern **BC15**	*Cavern* BC17	**Cavern BC18**	Cavern **BC19**	**Cavern BC20**	Cavern **WH105**
1	0.0090	0.0081	0.0067	0.0103	0.0064	0.0026
2	0.0086	0.0078	0.0064	0.0095	0.0058	0.0026
3	0.0076	0.0072	0.0057	0.0083	0.0050	0.0025
4	0.0067	0.0065	0.0050	0.0075	0.0045	0.0024
5	0.0060	0.0059	0.0046	0.0071	0.0042	0.0022
6	0.0055	0.0054	0.0042	0.0069	0.0040	0.0021
7	0.0051	0.0051	0.0040	0.0067	0.0039	0.0020
8	0.0049	0.0049	0.0039	0.0065 .	0.0038	0.0019
9	0.0047	0.0047	0.0038	0.0064	0.0037	0.0019
10	0.0046	0.0046	0.0037	0.0063	0.0036	0.0018
Two-Compound Parameters used in Eq. (4.3):						
ELTo ->	0.0040	0.0037	0.00335	0.0063	0.0036	0.0014
Cd **->**	0.0050	0.0044	0.00335	0.0040	0.0028	0.0012
fo **->**	1	1	1	1	1	1 GHz
fh **->**	3.2	4.0	3.0	2.0	20 .	6 GHz

4.3 **Model** for **EM** Losses in **Crude** Oil

Table 4.2 shows that the loss tangent of each crude oil **decreases** with increasing microwave frequency. The loss tangent of a dielectric is usually a constant. In some dielectric media, tan6 increases slightly with increasing frequency because the polar resonance absorption is centered at frequencies above S-band. The decrease observed in these crude oil is unusual and unexpected.

We offer an explanation for this unusual behavior of EM energy in crude oil in terms of polar molecules, such as the mercaptan class, having one or more absorption resonances located below s-band. The simplified model used here to fit the decreasing values of tan6 is called the two-compound model because the effective loss tangent ELT(f) of any particular crude oil mixture is represented by two terms, namely

$$ELT(f) = ELTo + Cd / (((f - fo) / fh)^2 + 1). \qquad (4.3)$$

These four parameters of the two-compound model are defined as:

ELTo = the constant tan6 due to EM absorption by one class of polar molecules whose absorption is heavily damped.
fo = the low resonance frequency of the second class of more lightly damped absorbers, probably certain mercaptans.
fh = the half width at half maximum absorption by this second set of compounds.
Cd = the peak value of tan6 due to this second set of compounds. Cd is proportional to their total concentration.

The values of these two-compound parameters which were used to generate the loss tangent values listed in Table 4.2 are given at the bottom of each column. The fact that this simple two-compound model fits our data to within the experimental uncertainties suggests that the main source of loss is only a subset of the sulphur compounds within the crude oil.

5. SUMMARY OF RESULTS

Microwave power transmission through samples of crude oil fron five SPR caverns at Bayou Choctaw plus one sweet crude from another SPR site has been observed at room temperature and one atmosphere. Each oil has been characterized by a value for its dielectric constant and a set of loss tangent values across the band from 1 to 10 GHz. A refined oil served to validate the multiple-reflection model of the sample holder to high precision.

The microwave loss tangents in the crude oils decrease strongly across this frequency range. This unusual frequency dependence is explained well by a simple two-compound model for the EM losses in crude oil. The precision of fitting is within the small experimental uncertainties.

Microwave losses are found to be lower in the sweeter crudes. Tentative correlation with chemical constituents suggests the some sulphur compounds, probably certain mercaptans, absorb strongly below 10 GHz.

Microwave losses are found to be low enough to give positive prospects for high-resolution radar mapping of SPR cavern walls.

6. CONCLUSIONS

6.1 Radar Napping of SPR Cavern Walls Appears Feasible.

Mapping SPR caverns with a resolution of a few feet at the cavern wall appears to be feasible. In fact, useful signal-to-noise at one GHz is apparently available in most SPR caverns according to the estimates being presented in a separate SAND report.7

6.2 Correlation with Sulphur Content Should Cut costs of Mapping.

Radar mapping within SPR caverns is now expected to give useful maps of most of the cavern walls. The next question now becomes which caverns are preferred candidates for a radar survey. The answer in terms of loss tangent values can be obtained by repeating the type of bench test reported here on samples of oil from the gallon samples taken for NIPER analysis. Once established, the correlation between loss tangent and certain of the sulphur compound concentrations will allow the regular NIPER tests to be an accurate screen for radar attenuation.

Therefore, it is recommended that 300-ml oil samples be taken for EM loss tests as companion samples to those taken for regular NIPER testing from SPR caverns whose oils cover the range of sulphur content from strongly sour to very sweet. Comparison of microwave loss, measured with the technique reported here, to the NIPER listings from a score of SPR caverns covering this range of sulphur concentration should establish the desired correlation.

7. ACKNOWLEDGEMENTS

The author is grateful to S. T. Wallace, 6257, for obtaining the crude oil samples and for checking the early calculations: to M. G. Armendariz, 2175, for arranging time on the automatic network analyzer and for instructions in its use: and to J. L. Todd, 6257, for stimulating discussions and for reviewing the logic and the algebra *of* the multiple-reflection models being used for the slotted-line sample holder. Errors and shortcomings that remain are the work of the author.

8. *REFERENCES*

1. K. L. Biringer, "Strategic Petroleum Reserve (SPR) Long Term Monitoring System Pressure Data Analyses," SAND87-0706, printed July 1987 by Sandia National Laboratories (SNLA), Albuquerque, NM 87185-5800.

2. Monthly Cavern Integrity Reports, prepared by PB-KBB, Inc. for Boeing Petroleum Services, Inc., New Orleans, LA 70123.

3. K. L. Biringer, "Strategic Petroleum Reserve Cavern Geotechnical Data Base," SAND84-1500, printed November 1984 by SNLA, NM 87185-5800.

4. W. R. Wawersik and D. H. Zeuch, "Creep and Creep Modeling of Three Domal Salts - A Comprehensive Update," SAND84-0568, printed by SNLA, NM 87185-5800.

5. J. K. Linn, "Sandia Laboratories Geotechnical Project Status," Monthly Report to DOE SPR PMO, dated January 31, 1988.

6. K. L. Biringer, "Status and Analysis of Sonar-in-Oil Project," Memo to J. K. Linn, 6257, SNLA, February 20, 1987.

7. J. G. Castle, "Radar Echo Strength Expected in Storage Caverns at the Strategic Petroleum Reserve," SAND88-3262, to be printed January 1989 by SNLA.

8. J. G. Castle, "Microwave Loss Observed in a Sweet Crude: Impact on Radar Demonstration," Internal Memo to J. K. Linn, 6257, SNLA, March 29, 1988, and "Echo Losses from Cavern Walls," Draft Technical Report to J. K. Linn, 6257, SNLA, March 28, 1988.

9. "Dielectric Materials and Applications," A. von Hippel, Ed., McGraw-Hill Book Co., 1948.

10. "Measuring Dielectric Constants with HP8510 Network Analyzer," HP Product Note No. 8510-3, Hewlett Packard Co., August 1985.

11. "Coaxial and Waveguide Measurement Accessories Catalog," Hewlett Packard Co., November 1986, p. 87.

12. J. K. Fitzpatrick, "Automatic Network Analysis Accuracy," Microwave System News, May 1980, p. 77-93.

13. "Reference Data for Radio Engineers," Sixth Ed., ITT-Howard Sams Co., 1981. ISBN: 0-672-21218-8.

14. J. D. Kraus and K. R. Carver, "Electromagnetics," 2nd Ed., McGraw-Hill Book Co., 1973, p. 402.

15. ibid., p. 332ff.

16. P. Debye, **Polar Molecules," Chapter 5, Chemical Catalog Co., NYC, 1929.

17. ref. 14, p. 346.

18. E. R. Pounder, "Physics of Ice," Pergamon Press, NYC, 1965, p. 129.

19. E. R. Beringer and J. G. Castle, "Microwave Magnetic Resonance Absorption in Oxygen," Phys. Rev., Vol. 81, p. 82ff, 1951.

20. **Microwave Designers' Handbook," 3rd Ed., Microwave System News, Vol. 15, No. 8, May 1985.

APPENDIX At EXPERIMENTAL PROCEDURE0 AND RESULTS

Appendix A presents the graphs of observed microwave power transmission and reflection as recorded by an automatic network analyzer ANA for the oil-filled slotted coaxial line[11] following a brief description of the procedures used to extend the sensitivity well beyond the manufacturer's stated limit.

A.l. Experimental Procedures

A.l.l Bench Equipment Used

A.1.1.1 Automatic Network Analyzer (ANA)

The ANA, Model HP8510B, is regularly calibrated and used for critical evaluation of high-reliability microwave devices across the frequency range from 0.5 GHz to 18 GHz. Therefore, the principal calibration uncertainty for this work derives from the normal step-by-step calibration procedure used at the start of each day's operation.12

A.1.1.2 Sample Holder

The coaxial slotted line, Model HP816A-011, was chosen for these tests from the stock available. The open slot allowed easy filling, emptying and cleaning, after the bottom seam was sealed up with plumbers' epoxy so as to hold liquids.11

The geometry of the HP816A-011 slotted line is summarized in Table A.1.1.2. The overall length is 24.8 cm. At each end is an APC-7 connector. Next to the connector is a 0.3-cm thick ferrite bead, which serves as support of the 0.30-cm diameter brass rod that forms the coaxial center conductor. The ferrite is assumed to have a dielectric constant of 20 and has an unknown loss tangent, whose value is fixed by the ANA observations with air filling.

Table A.1.1.2. Dimensions of Slotted Line Model HP816A-011.
Internal cross sections are all coaxial. The center conductor and outer conductor surfaces give a 50-ohm line impedance when air is the medium in the central sections. Interfaces are abrupt.

Section Label	Shape, Dielectric	Length cm	Description
APC-7	Circular, solid	0.4	Connector for coaxial cables to MA port number 1.
Bead	Circular, ferrite	0.3	Support for brass rod, 0.3-cm diameter.
Transition	Circular, air/oil	2.8	Al housing transition to flat plate coaxial section.
Slotted (central)	Flat plates air/oil	17.8	Plate separation = 0.54 cm, open sides.
Transition	Circular, air/oil	2.8	Al housing transition to flat plate coaxial section.
Bead	Circular, ferrite	0.3	Support for brass rod, 0.3-cm diameter.
APC-7	Circular, solid	0.4	Connector for coaxial cables to ANA port number 2.

The HP816A holder was designed to be operated with air filling most of the coaxial chamber between beads (23.4-cm long) and shows very low reflections with only air in it. Clearly, the reflections at each interface have been very well minimized for a 50-ohm characteristic line impedance.

Inserting -30 milliliters of oil raises the dielectric constant in the chamber and gives a strong reflection at each end due to the impedance mismatch. The multiple-reflection model used in this test report takes advantage of the pair of reflections at the two oil-bead interfaces being much larger than the other reflections. The calculation includes all the multiple reflections that contribute as much as .02 dB to the calculated $|S_{21}|^2$. A summary of the model is given in Appendix B.

A.1.1.3 Sensitivity of ANA Measurements

Product Note 8510-3, entitled, **Measuring Dielectric Constant with the HP8510 Network Analyzer," contains a useful description of the theory needed to interpret S-parameter data in terms of the dielectric permittivity of the medium:[1]

$$\varepsilon_r = \varepsilon_r' - j\,\varepsilon_r'' = \varepsilon_r' (1 - j \tan\delta).$$

The HP note states the accuracy of automatic measurement of ε_r' as -1 per cent and of ε_r'' as $\pm$ 0.02 for solid samples.10 The corresponding uncertainty in tan6 is $\pm$ 0.01 for ε_r' near 2. The manufacturer makes no claim for accuracy of loss tangents below 0.1.

On the other hand, the ANA can reproducibly measure transmission loss as small as 0.01 dB. The stability is better than that: after a full day's operation, the remnant loss (drift) in the ANA system with the sample holder removed has the root mean square (RMS) value of -0.0002 dB across 1 to 11 GHz. An incremental loss of 0.01 dB within the HP816A holder is produced at 1 GHz by changing the loss tangent of the liquid by -0.0001. So, we set the goal of our procedures and analysis to be the reduction of the tan6 uncertainty from the stated limit of 0.01 to an uncertainty near 0.0002 for liquids like crude oils.

A.1.2 Lab Procedures

A.1.2.1 Reproducible $|S_{21}|^2$ Values

The principal precautions taken included:

1. Avoiding polar contaminants within the sample holder.
2. Reducing bubbles in each oil sample to stable ones. This normally involved repetitions after waiting 20 minutes.
3. Confirming that the observed $|S_{21}|^2$ values are stable across the band to within the limit of 0.02 dB.
4. Recording the $|S_{11}|^2$ sweep for the final $|S_{21}|^2$ record.
5. Establishing the equality of $|S_{21}|^2$ and $|S_{12}|^2$ for each.
6. Confirming sufficient oil removal by observing $|S_{21}|^2$ for air after each cleaning.

A.1.2.2 Sequence for Low-Loss Liquids

The procedure started with ANA measurements on the empty holder in order to 'calibrate' out its losses across the same frequency band. Since cleaning without adding loss from polar solvents was difficult, this empty holder calibration was done after cleaning before each new sample of oil. Typical results are displayed in the figure in Section A.2.1.

Comparison of MA data on sweet crudes to the data on a widely available oil with a very low loss is the cornerstone of confidence in the calculated tan6 values. We chose the extra heavy, laxative-grade mineral oil (LAX) as our standard for low loss because it is widely available to others. LAX turned out to have a sufficiently low tan6 to give us strong confidence in our model for the holder losses and reflections. The holder model yields high precision for the **permittivity** values used to fit the observed transmission.

The sequence for taking data for each oil followed the cautions listed in Section **A.1.2.1** above. Reproducible $|S_{21}|^2$ values from 1 to 10 **GHz** to within 0.02 **dB** were obtained and then the corresponding $|S_{11}|^2$ plotted.

A.2. ANA Records of $|S_{11}|^2$ and $|S_{21}|^2$

A.2.1 Observations on Air-Filled Slottsd Lins

Observations on the air-filled **HP816A** line before any liquids had been inserted showed return loss below 40 **dB** and the transmission declining smoothly (no dips as large as **.02 dB**) from $|S_{21}|^2$ = -0.05 **dB** at 1 **GHz** to -0.25 **dB** at 10 **GHz.** Measurements on the air-filled line were repeated after each oil sample had been removed and the line cleaned without using solvents. Late in this series, we found that a Freon cleaning spray gave better cleaning and did not contribute measurable loss.

A.2.1.1 Reflected Microwave Power, Air Filling

The $|S_{11}|^2$ values for the slotted line filled with air after cleaning were below 20 dB. The pattern of dips in reflected power has a very constant period of 0.636 GHz ± 0.006 GHz, showing that the two air-bead interfaces, 23.4 cm apart, have much stronger reflection than any of the other interfaces.

A.2.1.2 Transmitted Microwave Power, Air Filling

The $|S_{21}|^2$ of the slotted line filled with air after reasonably thorough cleaning with paper and Freon spray is shown in Figure A.2.1.2. Values of the locus of the transmission peaks (TP) in this figure are listed in Table A.2.1.2.

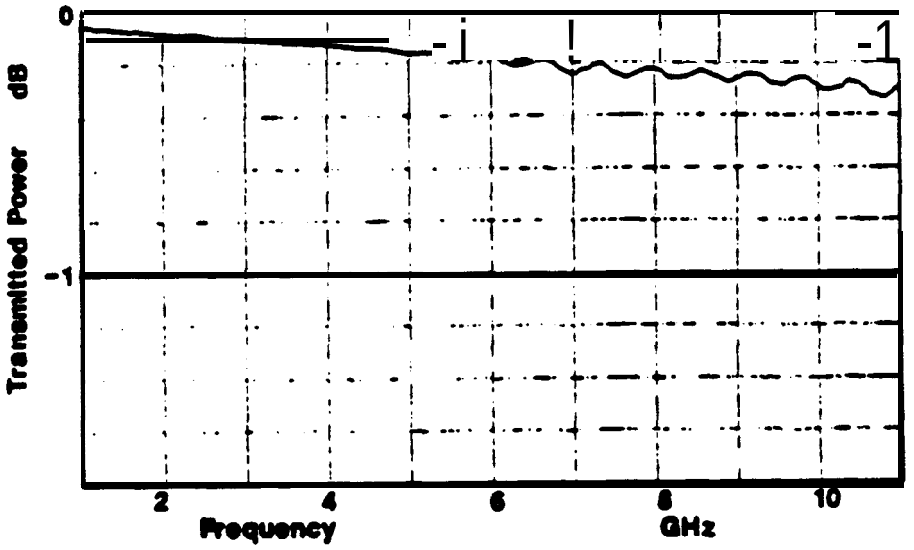

Figure A.2.1.2. Power Transmission, Air Filling.

The slight dips in transmission appearing above 5 GHz are due to oil films at ferrite bead surfaces left after Freon spraying.

Table A.2.1.2. Locus of Transmission Peaks (TP) with Air
TP values were read from trace of the peaks observed in the $|S_{21}|^2$ plot shown in Figure A.2.1.2.

Frequency GHz	*TP* **dB**
1	0.052
2	0.080
3	0.108
4	0.125
5	0.148
6	0.173
7	0.194
8	0.219
9	0.240
10	0.261

A.2.2 **Observations** on Low-Loss **Refined** Oil

The clear laxative-grade mineral oil LAX observations are shown in Figures A.2.2.1 and 2. Features include:
1. A constant period for the dips of 0.45 **GHz.**
2. Stable modulation of the dips with a period of 4.2 GHz.
3. Peaks in transmission indicating low loss.

The locus of the peaks is listed in Table A.2.2.

The dips show the periodicity expected from an oil with ε_r' = **2.1+** filling the **23.4-cm** space between ferrite beads. Other reflecting interfaces have smaller reflection coefficients and produce "modulation" of the primary dips. The frequency span of 4.2 **GHz** observed for the modulation in Figures A.2.2.1 and 2 corresponds to a pair of reflecting interfaces located at 2.5 **cm** from each ferrite interface. We interpret these interfaces as due to stable bubbles of trapped air in the analysis in Appendix B.

Table A.2.2. Locus of TP on Low-Loss Refined oil LAX

Frequency GHz	LAX dB
1	0.085
2	0.140
3	0.190
4	0.240
5	0.280
6	0.310
7	0.345
8	0.380
9	0.420
10	0.455

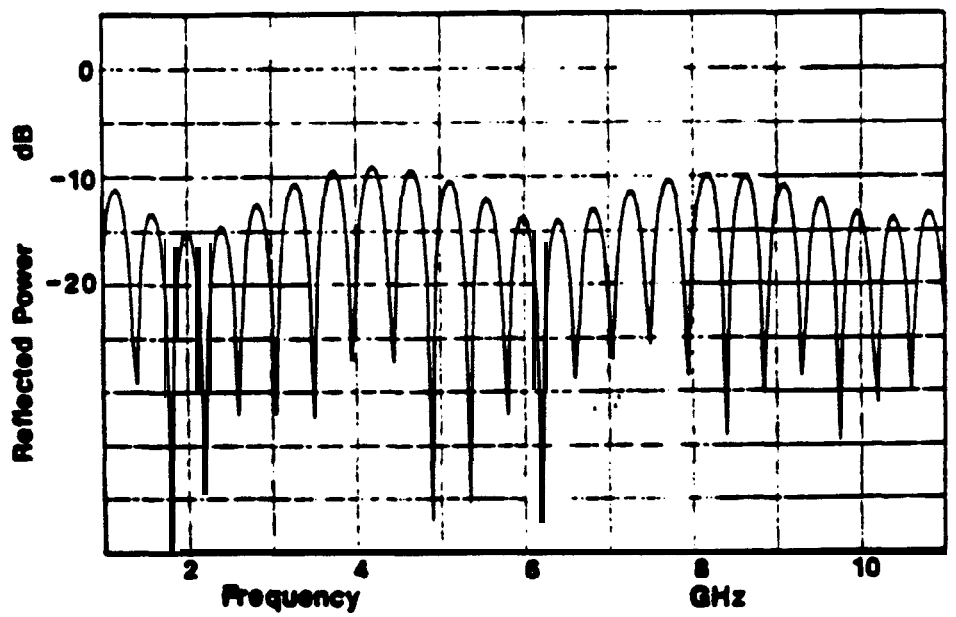

Figure A.2.2.1. Reflection with Refined Oil LAX.

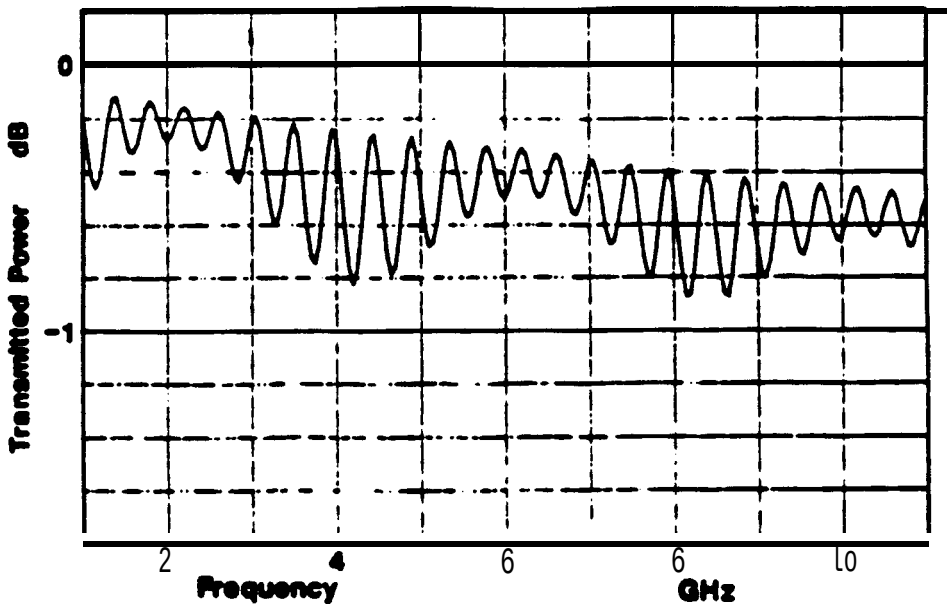

Figure A.?.?.?. **Transmission** with Refined Oil LAX.

A.2.3. Observations on Samples of Crude Oil

A.2.3.1. Microwave *Power* Reflected with Crude oils

The $|S_{11}|^2$ values recorded with six SPR crude oils are plotted in Figures A.2.3.1.106. The values found for $\varepsilon_r'_{oil}$ from the period *of* the dips evident in each figure *are* listed in Table 4.1 in the text.

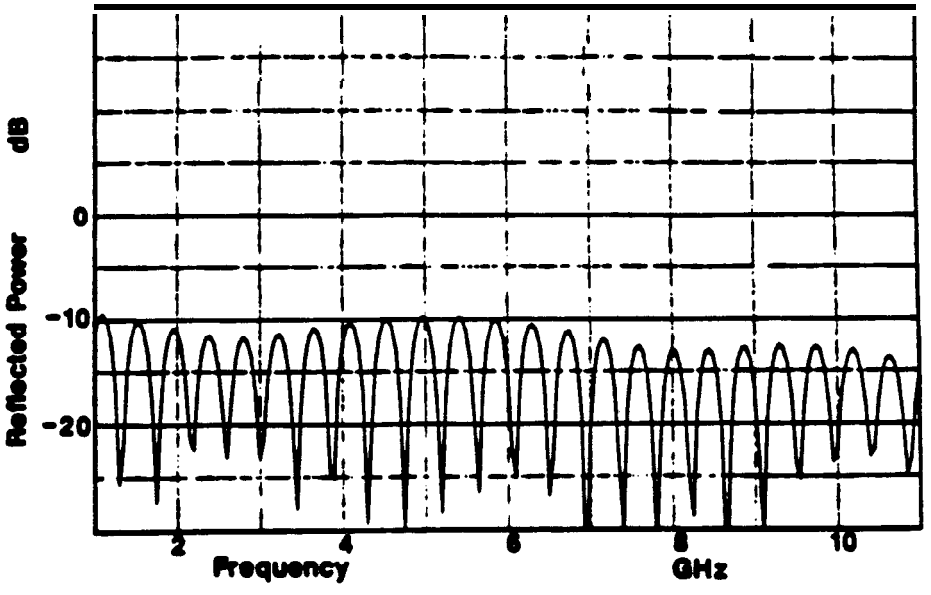

Figure A.2.3.1.1. Power Reflection with Oil From SPR Cavern BC15.

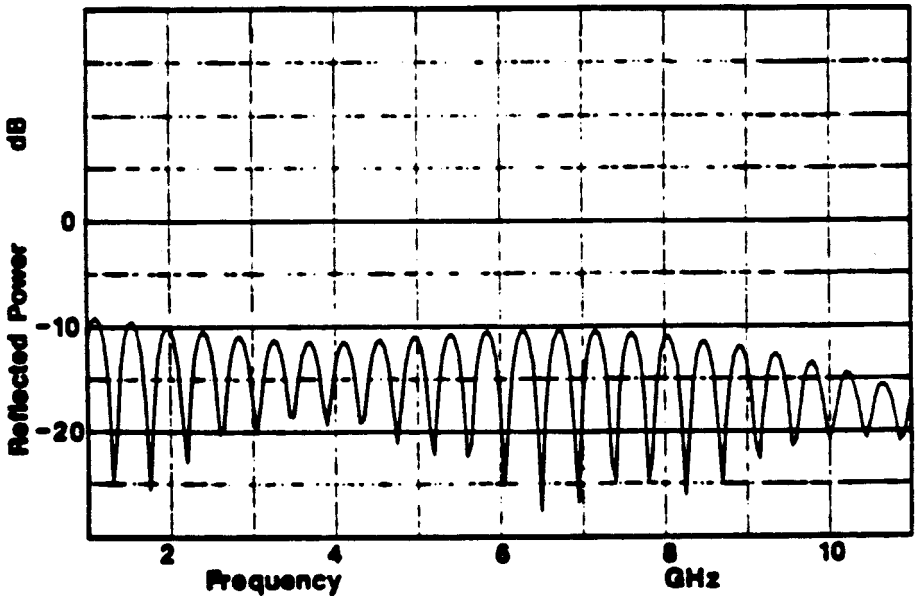

Figure A.2.3.1.2. Power Reflection with Oil From SPR Cavern BC17.

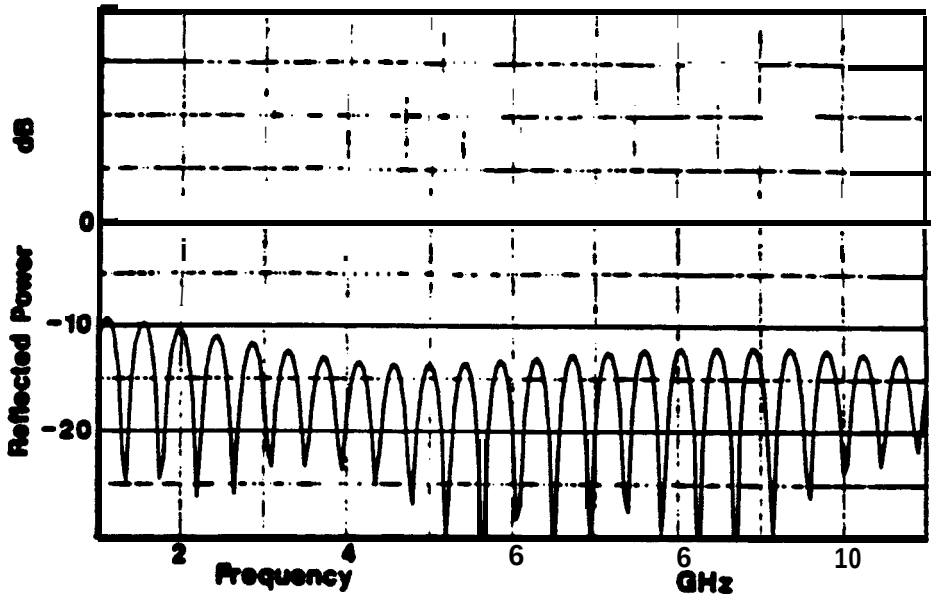

Figure **A.2.3.1.3.** Power Reflection with Oil From **SPR** Cavern BC18.

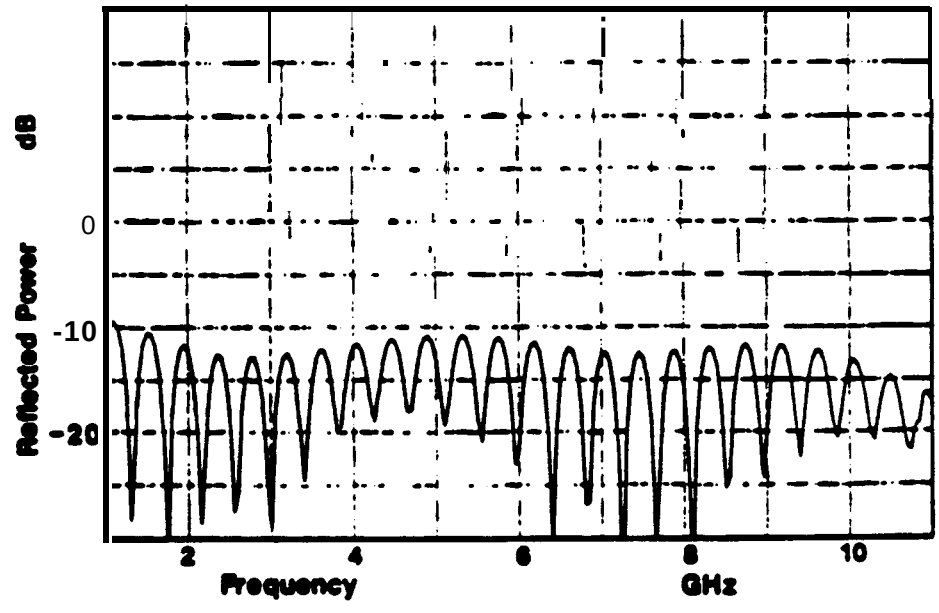

Figure **A.2.3.1.4.** Power Reflection *with* Oil *From* **SPR** *Cavern* **BC19.**

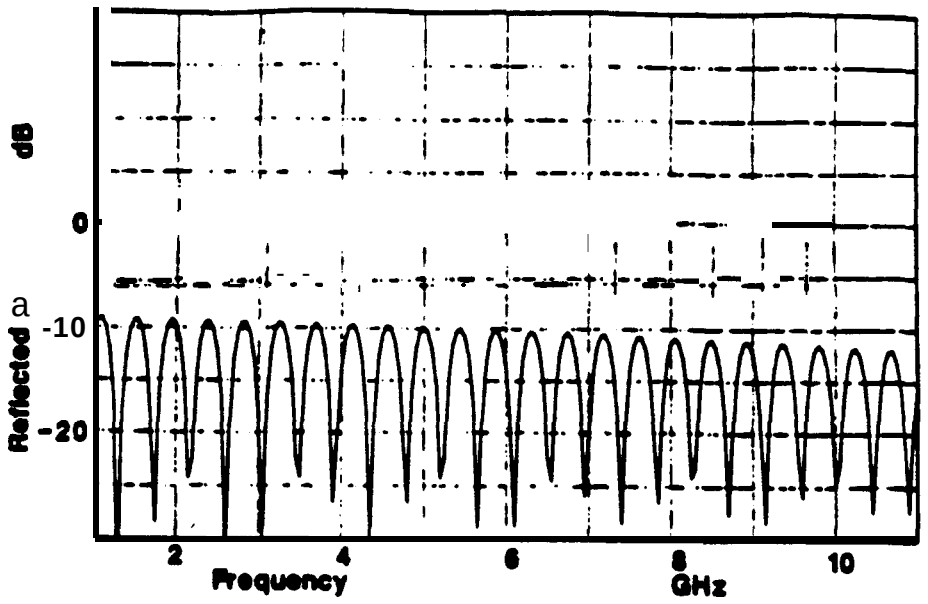

Figure *A.2.3.1.S.* Power Reflection with Oil *From* SPR Cavern BC20.

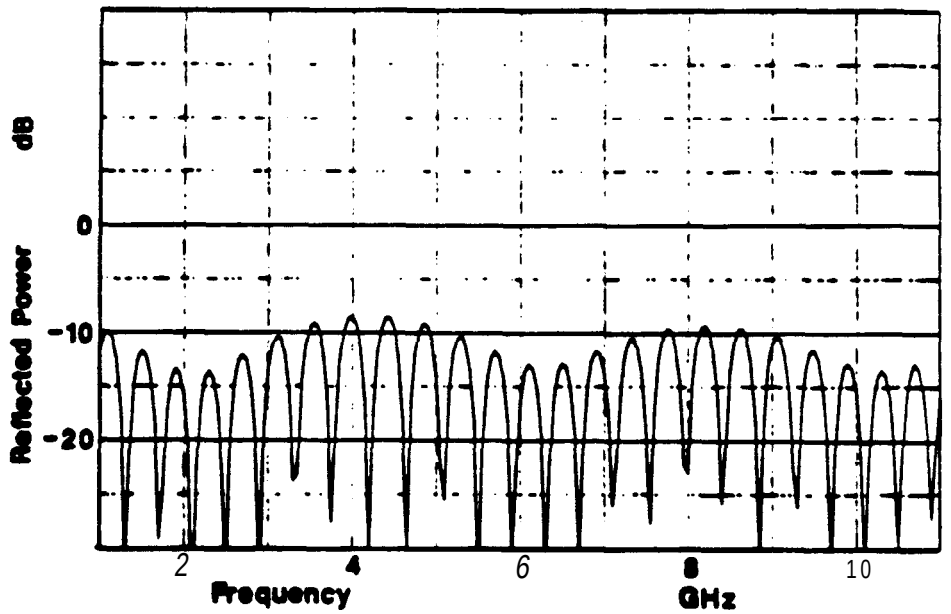

Figure **A.2.3.1.6. Power** Reflection with Oil From SPR **Cavern WH105.**

All

A.2.3.2. Microwave Power Transmitted with SPR Crude Oils

The $|S_{21}|^2$ values recorded with six crude oils from SPR are plotted in Figures A.2.3.2.106. The locus of the maxima in the observed $|S_{21}|^2$ is listed for each of the six crudes from f = 1 to 10 GHz in Table 3.4 in the body of this report. The samples from BC18 and BC20 show the least EM loss among the Bayou Choctaw crudes tested.

The lowest losses in the six samples of crude oil tested in this study are found in the sample WH105. Its viscosity resembles that of blackstrap molasses.

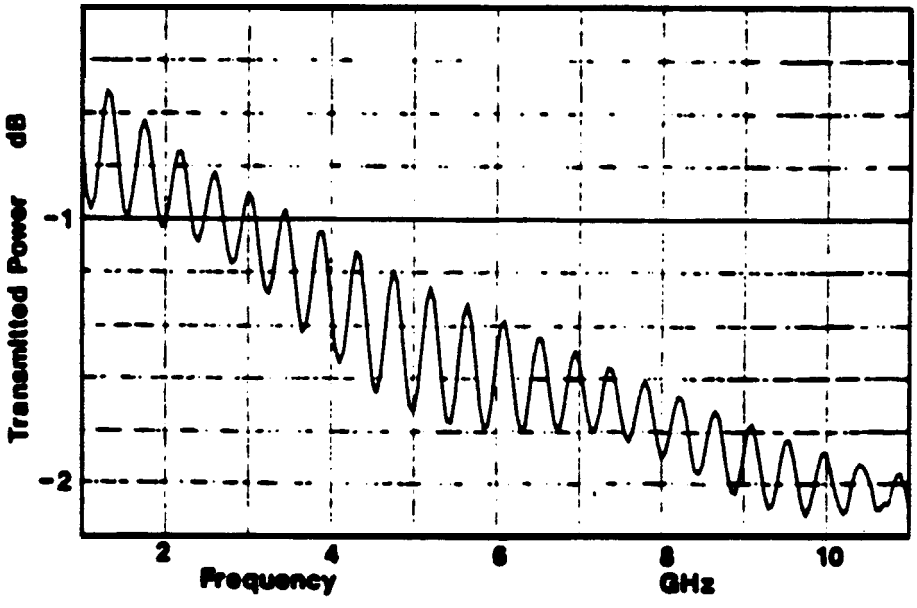

Figure A.2.3.2.1. Transmission with Oil From SPR Cavern BC15.

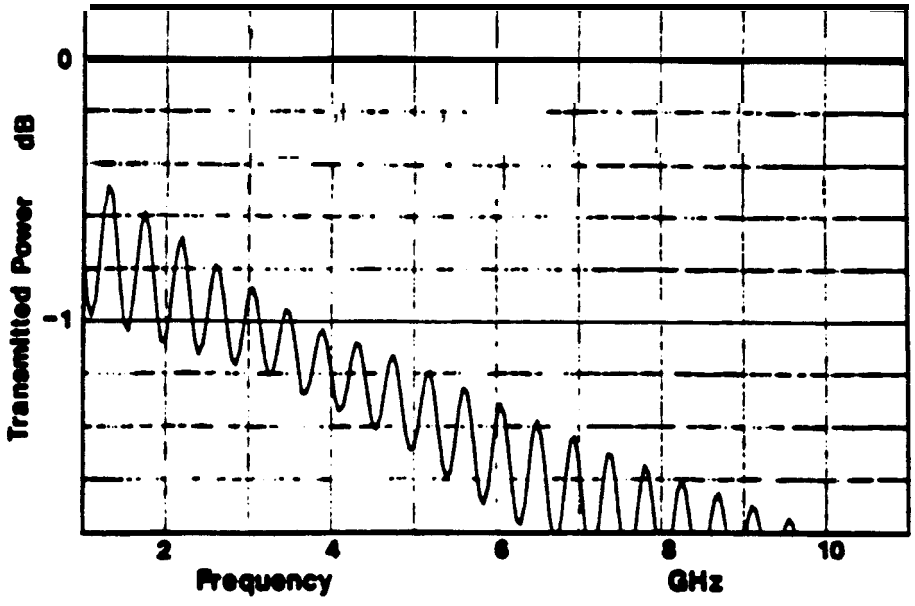

Figure A.2.3.2.2. **Transmission** with Oil From **SPR** Cavern BC17.

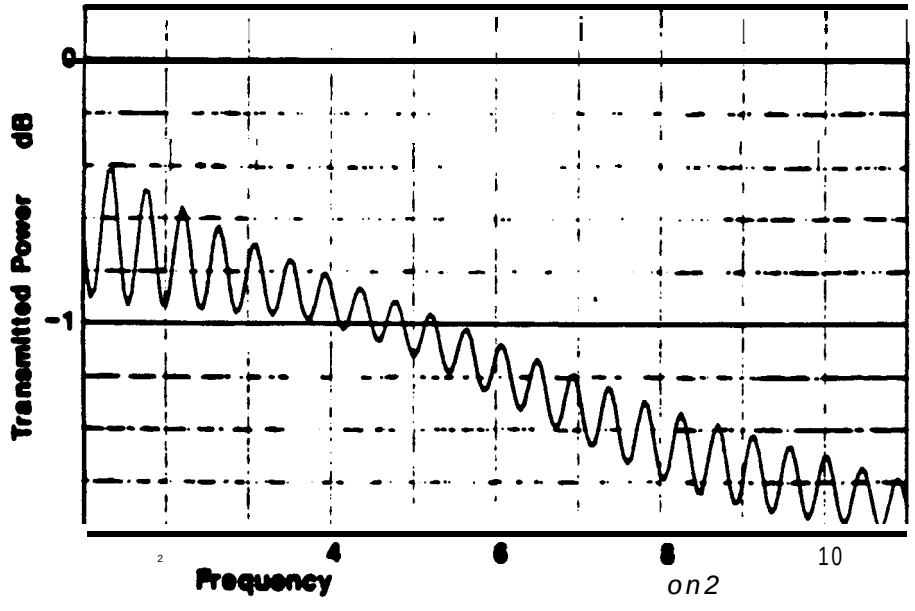

Figure A.2.3.2.3. Transmission with Oil *From* **SPR Cavern BC18.**

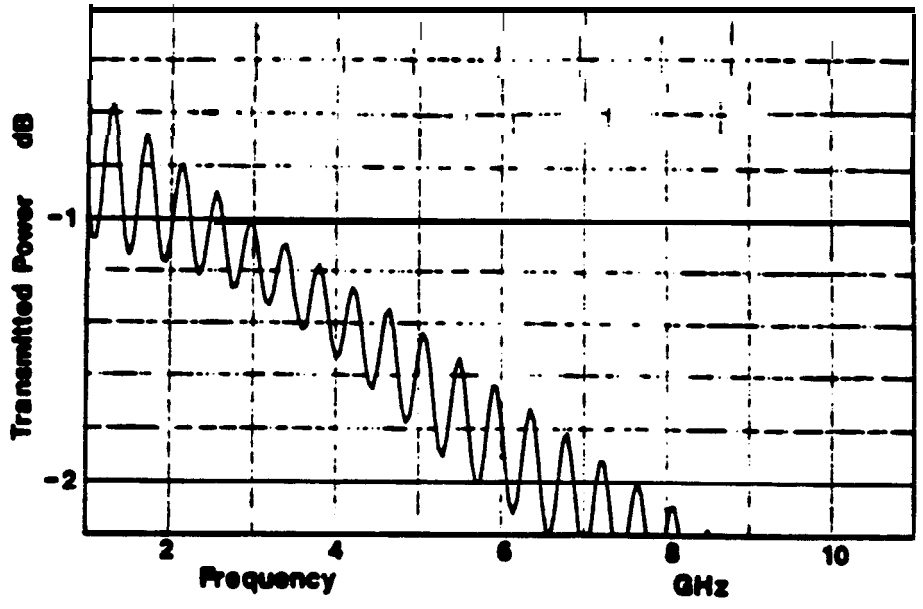

Figure A.2.3.2.4. **Transmission with** Oil **From SPR** Cavern **BC19.**

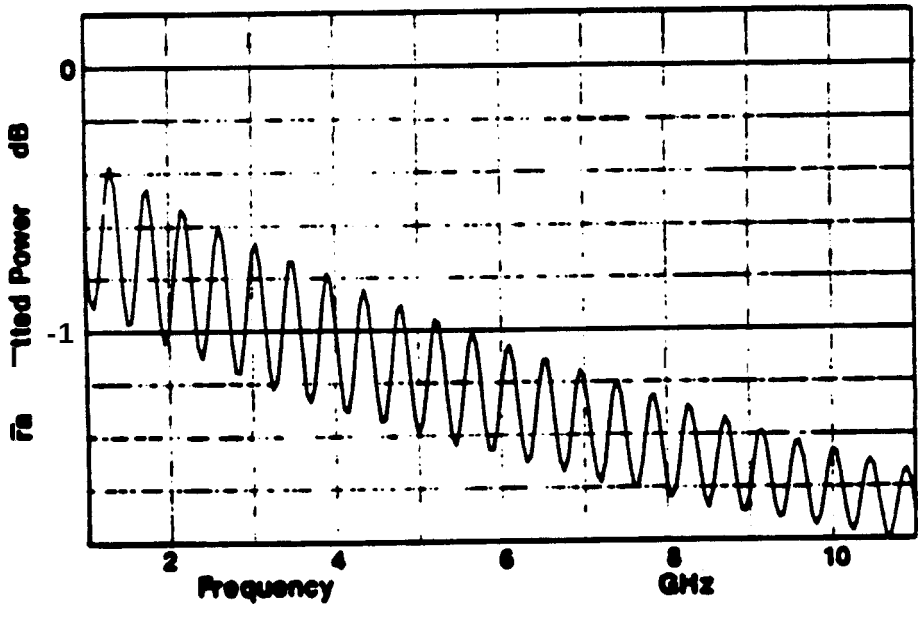

Piguro A.2.3.2.3. **Transmission** with Oil *From* **SPR Cavern BC20.**

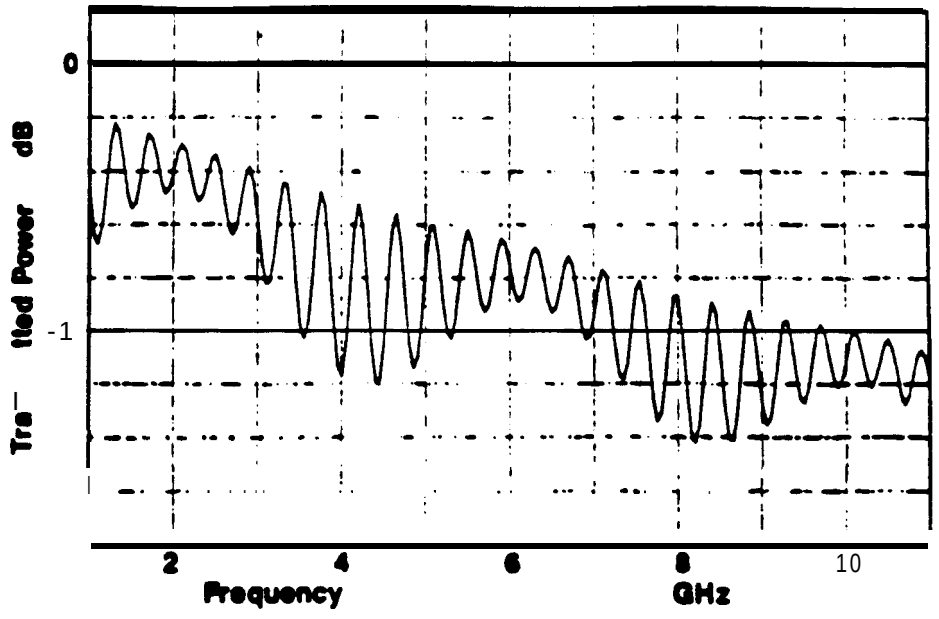

Figure A.2.3.2.6. Transmission with Oil From SPR Cavern **WH105.**

APPENDIX B: ANALYSIS OF OBSERVATIONS WITH SLOTTED LINE

B.l. Models Used

B.1.1. Zero Reflection Model

The goal of this analysis is to get values for the microwave loss tangent for each oil sample with reasonable accuracy. An analysis that is quick and adequate for liquids with large losses is to approximate the locus of the maxima in $|S_{21}|^2$ by the expression for the transmission coefficient from Reference 10 multiplied by the loss due to conduction currents in the coaxial surfaces within the holder. For large $\tan\delta$, the locus of the maxima in $|S_{21}|^2$ versus *frequency* (TP) would then be given in dB by

$$TP = 10 \log(\exp(-2 \pi N_i \tan\delta) \exp(-AO\ L_i\ (\varepsilon_r'_{oil}\ f)^{1/2})),$$

where N_i = number of wavlengths within the length L_i,
L_i = 23.4 cm,
AO = 4.53-4 per cm $GHz^{1/2}$ for the half brass, half aluminum coaxial line, and
$\varepsilon_r'_{oil}$ is fixed by the observed period of the dips in $|S_{21}|^2$ or in $|S_{11}|^2$.

$\tan\delta$ is the only adjustable parameter to fit this expression to the observed values of TP.

However, for the low loss tan6 values of interest for radar ranging beyond 100 feet, the multiple reflections contribute to the observed TP values and would cause uncertainty in any small $\tan\delta$ values calculated with the above expression. Therefore, we have set up a simplified model of the holder by assuming symmetry in the reflection coefficients. We calculate the vector sum of all the significant multiple reflections from the three pairs of interfaces. We find the bead-APC7 interface has a reflection coefficient no larger than 0.01; the flat-to-round interface, too small to be detected: and, for the thicker oils, a third pair of

reflectors occurring at air bubbles trapped against the beads. Fitting with this model for the holder yields precision even for the low values of $\tan\delta$ to within the experimental uncertainty.

Given this confidence in the fitted tan6 values, their unexpected decrease with frequency is explained here by a new model for microwave absorption involving molecular resonance absorption frequencies below S-band and modest collision damping from some of the sulphur compounds within the crude oils. Nearly half of the EM absorption comes from the usual highly damped absorption which is described by **ELTo,** the portion of the tan6 that is constant across the frequency band.

B.1.2. Model *for* **Losses** and Reflections in Holder

The known properties of the holder are used in this report as given quantities in the process of analyzing the ANA data on crude oils to get the loss tangent values. The approximate expression for TP given above is used as the exact expression for the transmission coefficient of each **section** within the holder between reflecting interfaces. Actual lengths are used: adjustments are made only for trapped air bubbles if they are present.

The unknown properties of the **HP816A-011** holder include:

1. The loss tangent of the ferrite - probably < 0.01.
2. The reflection coefficients of the internal interfaces.

Values for these unknowns are determined from the ANA data with air filling. We use the book value for AO. The values for the holder are then used as fixed inputs to the analysis for oil permittivity.

B.1.3. Model for **Microwave** Absorption in Oil

Inspection of the recorded $|S_{21}|^2$ graphs or the TP listed in Table 3.4 shows that the derivative of TP with respect to frequency decreases strongly from 1 to 10 **GHz.** The slope is twice as large at 2 **GHz** as it is near 9 **GHz** for every crude sample except **WH105,** where the decrease is only a factor of 1.5. This unusual behavior in crude oils needs an explanation.

Recall that in gases, where dipolar resonance absorption is not broadened so severely by molecular collisions,[19] the resonances involving dipoles containing oxygen and hydrogen are located above the microwave range.[20] The lowest resonance absorption is near 24 GHz for H_2O. In these gases, the collision damping broadens the resonance absorption and produces a loss tangent which rises with increasing microwave frequency. If there were a gas of dipoles having larger partition functions, the resonance frequencies could be lowered into and below S-band. Then, the loss tangent would decrease with increasing probe frequency across S-band. The model presented here nominates the mercaptan class (sulphur alcohols) which includes polar molecules with large partition functions. The model also uses the standard Lorentz broadening expression to calculate the loss tangent values versus frequency.

B.1.4. *Two-Compound* Model for Oil

Some of the polar molecules present as a dilute constituent of crude oil could behave like a "gas" of electric dipoles buffered by non-polar aliphatic molecules. We name our simple model for EM loss in oil as the two-compound model, associating one polar chemical compound or set of polar compounds as the dilute dipolar "gas" buffered by the non-polar diluents, and associating a second type of polar compound having much more damping and therefore with a constant loss tangent.

Prime candidates for the type of polar compound with a low resonance frequency, fo, are the mercaptans in these crudes. The simplest mercaptan, methyl thio-alcohol, is the analog of methyl alcohol with the oxygen atom replaced by a sulphur atom. We recognize that there may be many polar compounds with low resonance frequencies in a crude oil. For example, some aliphatic mercaptane are probably within the mercaptans detected in the NIPER listings in Table 2.1.

Assume that the resonance absorption frequency, fo, of the dielectric hysteresis in the first type of polar compound "gas" is near 1 GHz, a factor of 20 below the K-band resonance in the water

molecule.[20] Assume that molecular collisions produce a term in the microwave power loss that has a Lorentz shape with a half width at half maximum, fh. The value of this half width, fh, will be taken as characteristic of the first type of polar species in a given crude oil sample. The Lorentz form of this term in the power loss through the oil-filled coaxial holder will be

$$D1\ f\ /\ (\ z^2 + 1\ ),$$

where $z = (\ f - fo\ ) / fh$ and D1 is a coefficient proportional to the concentration of the polar gas.

Since the effective loss tangent (ELT) decreases strongly as frequency increases from 1 to 10 GHz, tables of values of ELT versus f are required. We simplify this variation of ELT with frequency by tying it to a simple two-compound model for the absorption. The expression used for ELT(f) is given by the equation in Section 4.3 of the text. The fits obtained for this simple oil model are within experimental uncertainty.

B.2. Analysis for Empty Holder

$|S_{21}|^2$ of the empty HP816A holder, when calculated with values of $\varepsilon_r'_{air} = 2E\text{-}6$, $\tan\delta_{air} = 6E\text{-}4$, A0 = 4.5E-4 per $GHz^{0.5}$ per cm $\pm$ 10% and $\tan\delta_{bead} = 0.003 \pm 0.002$, fits the observed TP within the experimental uncertainty. An example of the quality of fit to the ANA record in Figure A2.1.2.1 above is displayed in Figure B2 as the difference of the calculated $|S_{21}|^2$ from the observed.

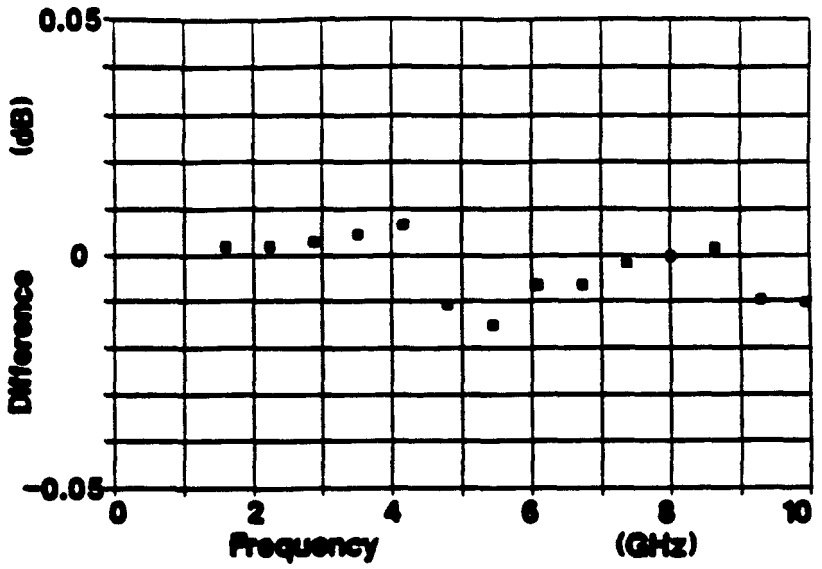

Figure 9.2. Test of Fit of Calculated $|S_{21}|^2$ for AIR.

B.3. Analysis for Low-Loss Refined Oil LAX

$|S_{21}|^2$ of the LAX-filled holder, when calculated with values of $\varepsilon_r'_{LAX} = 2.105 \pm .005$, $L_{bubble} = 2.47$ cm, the angle of bubble $= 0.3\ \pi \pm 10\%$, and $\tan\delta_{LAX} = 0.0004 \pm 0.0002$, fits the observed $|S_{21}|^2$ to within the experimental uncertainty of $\pm$ 0.02 dB. An example is given in the Figures B.3.1 and 2.

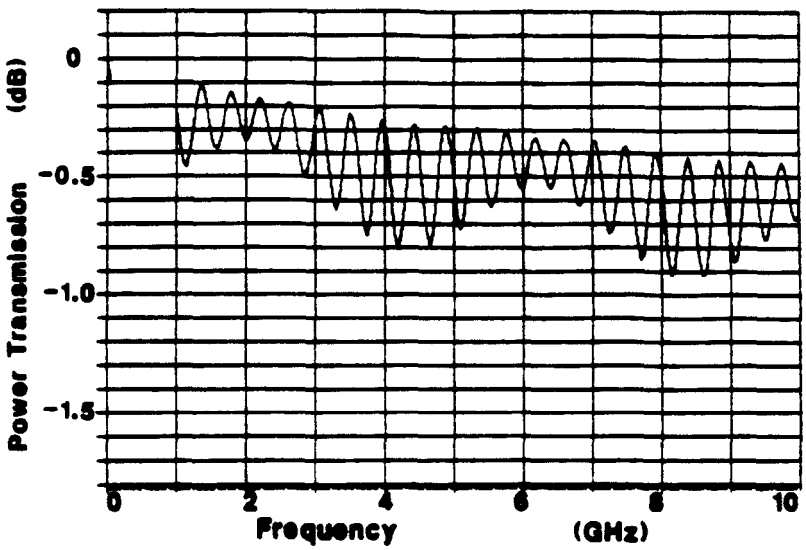

Figure **B.3.1. Calculated $|S_{21}|^2$** for Low-Loss Refined Oil.

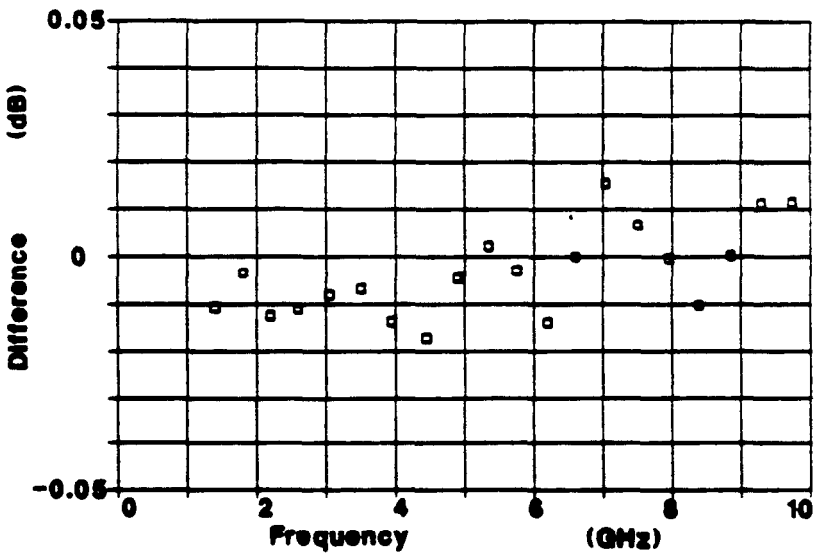

Figure B.3.2. Test **of** Fit of Calculated $|S_{21}|^2$ for LAX Oil.

B.4. Dielectric Constant and Loss Tangent for SPR Crude Oils

The only adjustable parameters used to fit the calculated $|S_{21}|^2$ to the observed transmission through a crude oil at each frequency are the loss tangent (ELT), the dielectric constant and the dimensions of any trapped air bubbles. The best-fit values for $\varepsilon_r'_{oil}$ are listed, along with their uncertainties, in Table 4.1 in the text. Best fit value8 for ELT(f) are listed in Table 4.2, along with the four parameters of the absorption model for each crude oil. The uncertainty in each ELT value is typically ± 0.0002 because a change of 0.0002 shifts the $|S_{21}|^2$ by 0.02 dB. The uncertainty in fh values is ± 0.5 GHz.

B.4.1 Quality of Fit for the Two-Compound Oil Model

The close fit of the two-compound oil model discussed above is apparent in the graphs of the difference between the $|S_{21}|^2$ calculated and the observed TP shown in Figures B.4.1.1-6. The differences fall within the uncertainty in the measured values.

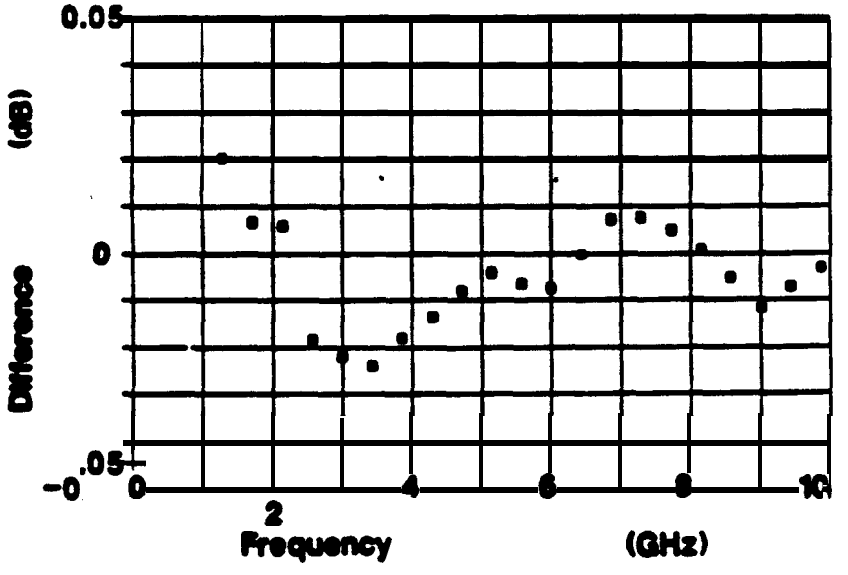

Figure B.4.1.1. Test of Fit in SPR Crude Oil from BC15.

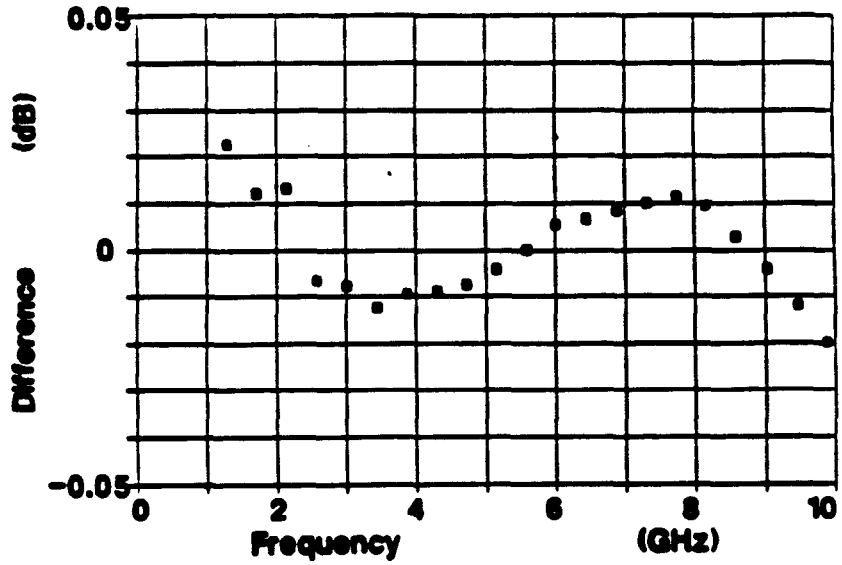

Figure B.4.1.2. **Test** of Fit in **SPR Crude** Oil from BC17.

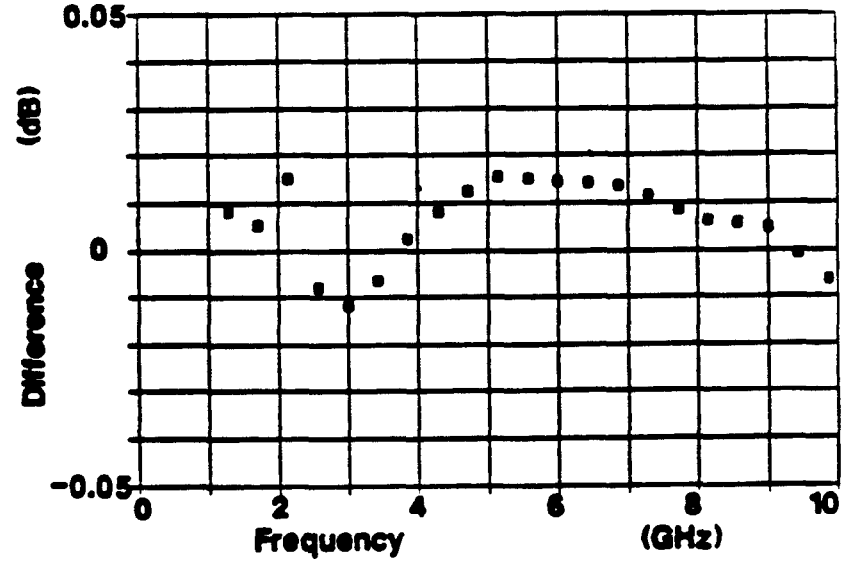

Figure B.4.1.3. Test of Fit in **SPR Crude** Oil from BC18.

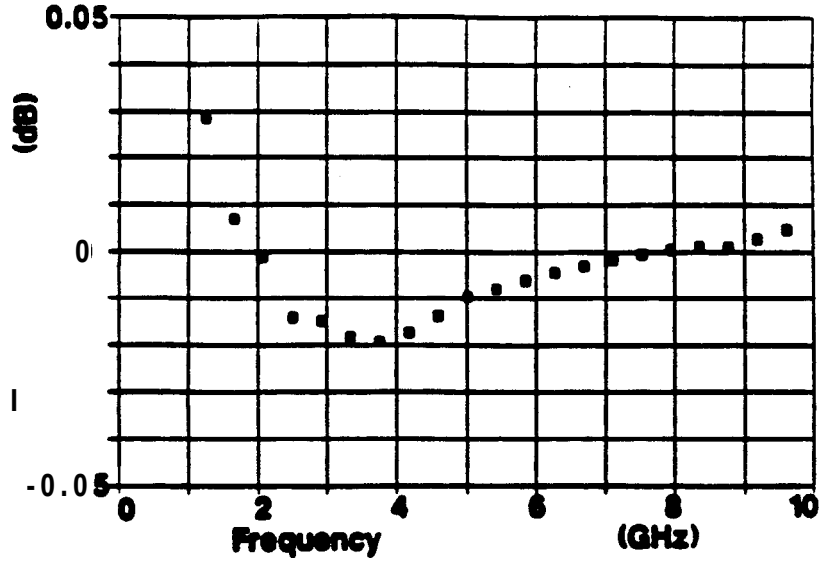

Figure B.4.1.4. Test of **Fit** in **SPR Crude** Oil from **BC19.**

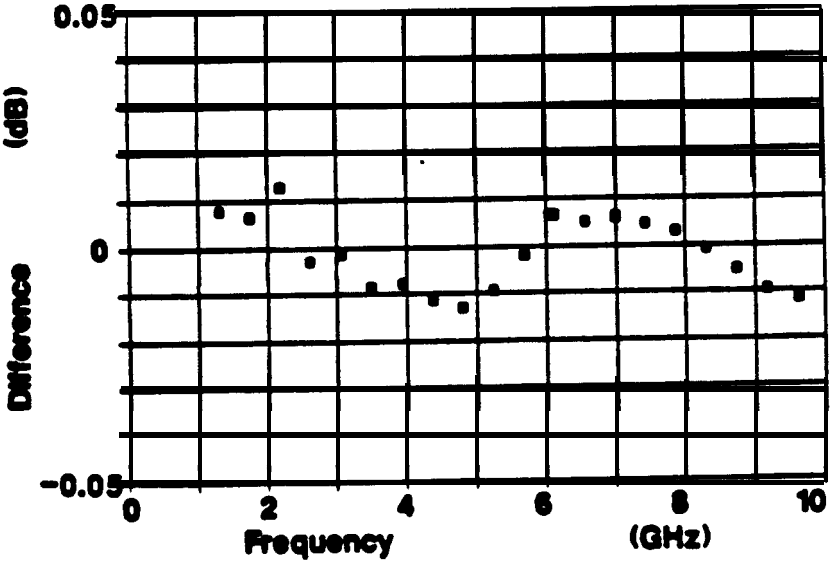

Figure B.4.1.5. Test of Fit in **SPR** Crude Oil from **BC20.**

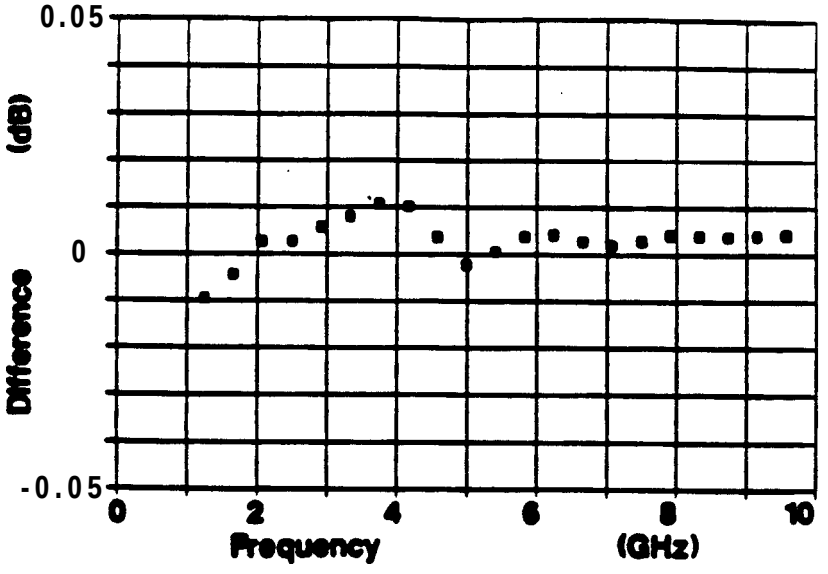

Figure B.4.1.6. Test of Fit in SPR **Crude** Oil from **WH105.**

Distribution of SAND88-1895:

U.S. DOE SPR PMO (9)
900 Commerce Road East
New Orleans, LA 70123
Attn: D. R. Spence, PR-62
E. E. Chapple, PR-622 (5)
D. W. Whittington, PR-622
TDCS (2)

U.S. Department of Energy (1)
Strategic Petroleum Reserve
1000 Independence Avenue SW
Washington, D.C. 20585
Attn: R. Smith

U.S. Department of Energy (1)
Oak Ridge Operations Office
P.O. Box E
Oak Ridge, TN 37831
Attn: J. Milloway

DOE SPR Bayou Choctaw Site (2)
P.O. Box 776
Plaguemine, LA 70764
Attn: J. M. Hyde, DOE
Box 1270,
Winnie, TX 77665
A. E. Fruge, DOE

DOE SPR Bryan Mound Site (1)
P.O. Box 2276
Freeport, TX 77541
Attn: C. Bellam, DOE

Boeing Petroleum Services (5)
850 South Clearview Parkway
New Orleans, LA 70123
Attn: J. Siemers (3)
K. Mills
T. Eyermann

Louisiana Geological Survey (1)
University Station: Box G
Baton Rouge, LA 70893
Attn: K. E. Ramsey

Solution Mining Research
Institute 812 Muriel Street
Woodstock, IL 60098
Attn: H. Fiedelman

Texas Bureau of Economic
Geology (2)
University Station, Box X
Austin, TX 78713
Attn: W. L. Fisher

Walk-Haydel & Associates, Inc.
600 Carondelet St.
New Orleans, LA 70130
Attn: Gary Trochesset

2174 M. G. Armendariz
2174 D. C. Martin
3141 S. A. Landenberger (5)
3154-l C. Ward,
FOR: DOE/OSTI (8)
3151 w. I. Klein (3)
6000 D. L. Hartley
6200 V. L. Dugan
6230 W. C. Luth
6231 H. C. Hardee
6232 W. R. Wawersik
6232 D. H. Zeuch
6250 R. K. Traeger
6252 J. Dunn
6257 J. K. Linn (10)
6257 J. G. Castle (15)
6257 S. L. Chavez
6257 K. L. Goin
6257 G. S. Heffelfinger
6257 J. T. Neal
6257 J. L. Todd
6257 S. T. Wallace
6257 S. W. Webb
8524 J. R. Wackerly